International Journal of Nanomedicine

Dovepress
open access to scientific and medical research

Open Access Full Text Article

ORIGINAL RESEARCH

Rifampicin conjugated silver nanoparticles: a new arena for development of antibiofilm potential against methicillin resistant *Staphylococcus aureus* and *Klebsiella pneumoniae*

This article was published in the following Dove Press journal:
International Journal of Nanomedicine

Umar Farooq[1,*]
Touqeer Ahmad[1,*]
Ajmal Khan[2]
Rizwana Sarwar[1]
Jazib Shafiq[3]
Yasir Raza[4]
Ayaz Ahmed[3]
Safi Ullah[5]
Najeeb Ur Rehman[2]
Ahmed Al-Harrasi[2]

[1]Department of Chemistry, COMSATS University Islamabad Abbottabad Campus, Abbottabad, Pakistan; [2]Natural and Medical Sciences Research Center, University of Nizwa, Nizwa, Sultanate of Oman; [3]Dr. Panjwani Center for Molecular Medicine and Drug Research, International Center for Chemical and Biological Sciences, University of Karachi, Karachi, Pakistan; [4]Department of Microbiology, University of Karachi, Karachi, Pakistan; [5]Department of Pharmacy, University of Peshawar, Peshawar, Pakistan

*These authors contributed equally to this work

Correspondence: Ajmal Khan; Ahmed Al-Harrasi
Natural and Medical Sciences Research Center, University of Nizwa, P.O Box 33, Birkat Al Mauz, Nizwa 616, Sultanate of Oman
Tel +9 682 544 6502;
+9 682 544 6328
Email ajmalkhan@unizwa.edu.om; aharrasi@unizwa.edu.om

Background: Infections caused by drug resistant bacteria are a major health concern worldwide and have prompted scientists to carry out efforts to overcome this challenge. Researchers and pharmaceutical companies are trying to develop new kinds of antimicrobial agents by using different physical and chemical methods to overcome these problems.

Materials and methods: In the present study, rifampicin conjugated silver (Rif-Ag) nanoparticles have successfully been synthesized using a chemical method. Characterization of the nanoparticles was performed using a UV-Vis spectrophotometer, FTIR, SEM, TEM, and AFM.

Results: The AFM, SEM, and TEM results showed that the average particle size of Rif-Ag nanoparticles was about 15–18±4 nm. The FTIR spectra revealed the conjugation of $-NH_2$ and –OH functional moiety with silver nanoparticles surface. Considering the penetrating power of rifampicin, the free drug is compared with synthesized nanoparticle for antimicrobial, biofilm inhibition, and eradication potential. Synthesized nanoparticles were found to be significantly active as compared to drug alone.

Conclusion: This study has shown greater biofilm inhibitory and eradicating potential against methicillin resistant *Staphylococcus aureus* and *Klebsiella pneumoniae*, as evident by crystal violet, MTT staining, and microscopic analysis. So, it will be further modified, and studies for the mechanism of action are needed.

Keywords: rifampicin, silver nanoparticles, TEM, AFM, antibiofilm, *Staphylococcus aureus*, *Klebsiella pneumoniae*

Introduction

The arena of nanotechnology has emerged with a wide range of applications in electronics,[1] cosmetics,[2] energy,[3,4] catalysis,[5,6] and medicines.[7,8] The diverse range of optical, chemical, and mechanical properties of the nanomaterial is related to its large surface area.[9–11] It is well known that controlling the particle size at nano scale can help to control the surface energy, surface area, and bring specificity in the mode of action of the synthesized material.[12,13] Nanoparticles alone are unstable because of high surface energy and small size, so they are stabilized with a suitable capping agent.[14–16] Nano drugs have been proved effective in treatment of dreadful diseases like cancer,[17] hepatitis,[18] and diabetes.[19] Nano medicines have a lot of advantages, like enhancement of absorption into tissues, selectivity in their mode of action, and improvement of intracellular tissues.[20,21] Some nano technology based drugs for

dreadful diseases are in trials, and some are commercially available on the market.[22,23] Nanomedicine offers many possibilities to improve diagnosis and therapy, and can tackle a series of diseases with more effectiveness and at an affordable price. Different types of metallic nanoparticles loaded with antibiotic were synthesized. Amongst the metallic nanoparticles, silver nanoparticles showed a pronounced effect against human immune deficiency virus type 1[24] and hepatitis B virus.[18] Efficiency, therapeutic value, and specificity of medicinal drugs increase with the formation of nanoparticles.[25–27] Different methods were employed for nanoparticles synthesis, among them a reduction of metal salt with inorganic reducing agent at high temperature was the most common method.[28–30]

Rifampicin is a semisynthetic, broad spectrum antibiotic used commonly for the treatment of tuberculosis.[31,32] However, this drug is used to treat various other bacterial infections, including Methicillin resistant *Staphylococcus aureus*.[33] After its discovery it shortened the period of TB chemotherapy as well as other chronic life-threatening bacterial infections with its penetrating power to deep tissues or living cells as well as its RNA polymerase inhibition activity. Due to its penetrating power, it is also reported to treat various biofilm-related infections.[34,35] With the passage of time, the emerging resistance among microbes, and considering its adverse effects, researchers have found different ways to improve its bioavailability with the least adverse effect.[36] Nanotechnology gives new worth to existing antibiotics by decreasing their size to nano level, which results in an increase in cell permeability. Recently, nanoconjugate of gentamicin and chlorhexidine showed better biofilm inhibition and eradication efficacy.[37,38]

In current research we reported facile synthesis of rifampicin conjugated silver nanoparticles (Rif-Ag-NPs) with slight modification in Tarkevisch method by using sodium citrate as a reducing agent. Rifampicin is a broad spectrum semi synthetic compound used for capping of silver nanoparticles. Seemingly the -NH_2 and -OH groups of rifampicin are responsible for stabilization of Ag nanoparticles. The antimicrobial, biofilm inhibition and eradication capability of synthesized nanoparticles were also evaluated.

Materials and methods

Material

Silver nitrate ($AgNO_3$) was purchased from Merck. Sodium hydroxide (NaOH), hydrochloric acid (HCl), and Sodium citrate were purchased from Sigma Aldrich. Antibiotics were procured from Abbot pharmaceutical company (Islamabad). Double distilled water was used throughout the experiment. A nanoparticles spectrum was logged on a UV-Vis spectrophotometer. The pH effect was checked using a pH meter (Oakton, Eutech) equipped with glass working electrode.

Synthesis of nanoprticles

Synthesis of rifampicin conjugated silver nanoparticles was carried out using Tarkevisch method.[39] Around 0.5 mM solution of silver nitrate was prepared by dissolving 21.23 mg in 250 mL of double distilled water. Similarly, 0.5 mM solution of rifampicin was prepared by dissolving 102.86 mg in 250 mL of methanol/water mixture because rifampicin has lower solubility in water. For the synthesis, first silver nitrate solution was boiled at 100°C then followed by the addition of drug (which acts as a capping agent) and sodium citrates. After addition of the capping agent and reducing agent, a change in solution color was observed, from reddish to dirty brownish.

Optimization of reaction was achieved by mixing different concentrations of metal to ligand. The concentration ratio (metal: ligand) that gave the best absorbance value was selected for nanoparticles synthesis. For recovery of nanoparticles, synthesized nanoparticles were centrifuged at 12,000 rpm for 15 minutes and followed by washing with double distilled water in order to remove excess reducing agent and antibiotic.

Stability of nanoparticles against pH

The pH meter with glass working electrode and reference KCl was used for measuring pH of nanoparticles. 0.5 M solution of sodium hydroxide and hydrochloric acid was prepared for checking the stability of nanoparticles against a different range of pH. Nanoparticles stability was checked in extreme acidic, basic, and neutral conditions.

Stability against brine solution

Nanoparticles stability was checked against different concentrations of brine solution. The resulting solution was kept at room temperature and, after 24 hours, UV-Vis spectra were recorded. An increase in peak intensity suggested these conditions were more favorable for growth of Rif-Ag-NPs.

Fourier transform infrared spectroscopy (FTIR)

FTIR spectral data was recorded to ascertain the presence of various functionalities present in the drug before and

synthesized silver nanoparticles. For analysis, the resulting suspension was washed with deionized water and was freeze dried. The FTIR spectra was recorded on an IR spectrophotometer (IR-460 Shimadzu, Kyoto, Japan).

Scanning electron microscopy (SEM)

For the confirmation of particle shape and surface morphology of silver nanoparticles, SEM analysis was performed. The samples were imaged in the SEM using a JEOL, JSM-6510LA, Analytical Scanning Electron Microscope model operated at 15 kV. For SEM examination, a small amount of synthesized metallic nanoparticles was placed on a carbon-coated grid at an operating voltage of 120 KeV.

Transmission electron microscope (TEM)

Various microscopy techniques are available for characterization of nanoparticles, however the transmission electron microscope (TEM) and scanning electron microscope (SEM) are arguably the most popular. The size and morphology of gold nanoparticles were confirmed by TEM (Model: JEOL, TEM-1400 Electron Microscope), operated at an accelerating voltage of 110 kV. The nanoparticles samples for TEM analysis were prepared by drop-coating the gold nanoparticles solution on carbon-coated copper grids.

AFM analysis

The size and morphology of the synthesized silver nanoparticles was determined by using an Atomic Force Microscope (Agilent Technologies 5500, USA) Agilent 5500 operated in tapping mode.

Bacterial strains and growth conditions

Klebsiella pneumoniae (ATCC: 13882), *Proteus mirabilis* (ATCC: 12453), *Streptococcus mutans* (ATCC: 25175), *methicillin resistant Staphylococcus aureus* (MRSA; ATCC: 43300), *Enterobacter aerogenes* (ATCC: 13048), and *Enterococcus faecalis* (ATCC: 29212) were used in this study. Except *S. aureus* and *S. mutans*, remaining strains were cultured or maintained in tryptic soya agar/broth (TSA or TSB) and MacConkeys agar (Oxoid, UK). MRSA and *S. mutans* were cultured in brain heart infusion (BHI) agar/broth (Oxoid) supplemented with 1% glucose and sucrose, respectively. All the strains were grown aerobically at 37°C for 24 hours.

Minimum inhibitory concentration (MIC)

Antimicrobial activity of the synthesized rifampicin nanoparticle was determined by using broth microdilution method by using a 96-well plate, as described before.[40] Standard drug and its synthesized nanoparticles were serially (2-fold) diluted Mueller Hinton broth (Oxoid) followed by addition of each bacterial lane in their respective wells at 5×10^5 CFU/mL. Each lane was supplemented with vehicle control (1% DMSO), positive control, and negative controls. Minimum inhibitory concentration (MIC) was noted after incubation for 24 hours at 37°C. The lowest concentration of compound which inhibited the growth was considered the MIC.

Biofilm inhibition potential of the compounds

Biofilm inhibiting potential of the standard Rifampicin drug and its nanoparticle was determined by using crystal violet method, as described previously.[38,41] Biofilm inhibition was evaluated by using the following equation:

$$\%\ \textbf{biofilm inhibition} = \{(\textbf{O.D. in control} - \textbf{O.D. of test})/\textbf{O.D. in control}\}\textbf{x 100}$$

Effect of compounds on biofilm viability

3-(4,5-dimethylthiazole-2-yl)-2,5-diphenyltetrazolium bromide (MTT dye) was used to evaluate the biofilm viability after treatment with rifampicin and its nanoparticle. Biofilm viability was determined in 96 well plate as described earlier by our group.[42] Briefly, after overnight incubation with drug and its nanoconjugate the spent medium was aseptically aspirated, washed and stained with 200 µL of 0.5 µg/mL MTT solution for 3 h at 37 °C. After incubation the formazon crystals formed due to metabolically active cells were dissolved in DMSO (200 µL) and A570 was determined using a microtiter plate reader (Tecan, Austria USA). Metabolic inhibition was computed by using following equation:

$$\textbf{Reduction in Viability}\ (\%) = \textbf{100} - (\textbf{OD treated at 570nm}/\textbf{OD control at 570nm})\textbf{x 100}$$

Eradication of established biofilm

The biofilm eradicating potential of the rifampicin and its nanoconjugate were determined by crystal violet method.[42] Briefly, overnight grown static biofilms of MRSA, *K. pneumoniae* and *S. mutans* were treated with different concentrations and incubated again overnight. Each lane was also supplemented with positive and negative controls. Biofilm eradicating potential was also

visualized microscopically by using a Nikon TE 2,000 Inverted microscope (Nikon, Japan).

Statistical analysis

For the analysis of data, the Student's *t*-test was utilized by using SPSS ver. 20 (IBM, USA).

Results

Nanoparticles alone are unstable because of their high surface energy.[43] Rifampicin, a broad spectrum antibiotic, was used as a capping agent to lower surface energy and to avoid the formation of nano aggregates (structure and capping ability was shown in Figures 1 and 2). Sulfur, hydroxyl, and amino groups are well known for formation of silver and gold nanoparticles. UV-Vis spectra of rifampicin conjugated silver nanoparticles showed a sharp peak at 330 nm, which is the characteristic of silver nanoparticles.

Reaction optimization

Nanoparticles were optimized using different metal-to-drug ratios, followed by addition of reducing agent. Rif-Ag-NPs were synthesized using a chemical synthesis method. In this method, silver salt solution was boiled, followed by addition of sodium citrate and capping agent (rifampicin). Upon addition, the solution color changes from reddish to dirty brownish, which confirms the synthesis of nanoparticles. The best optimized ratio was found to be 1:1 (metal: drug). The optimizing ratio at which UV-Vis absorbance was found to be maximum was considered for nanoparticles synthesis. With a further increase or decrease in metal salt or drug concentration, a decline in UV-Vis spectra was observed, which confirmed the instability or decomposition of nanoparticles. Reaction optimization of Rif-Ag-NPs has been shown in Figure 3.

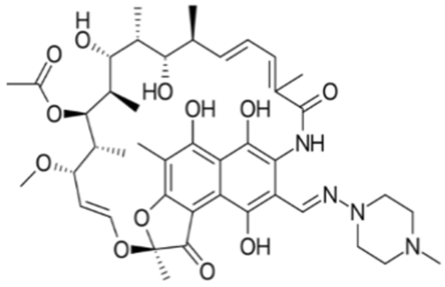

Figure 1 Structure of rifampicin.

Heat effect

The stability pattern for synthesized nanoparticles against different temperature, ie, 25°C, 50°C, 75°C, 100°C have been shown in Figure 4. Heat effect was checked to optimize best reaction conditions for the synthesis of nanoparticles. Higher temperature was selected for the synthesis because nanoparticle showed maximum absorption. Direct relation was observed between absorbance and temperature (elevation in temperature caused an increase in absorbance) due to increase in reaction kinetics. Increasing temperature leads to faster reduction of Ag^{+1} to Ag°. A temperature between 80–100ºC was considered an optimum condition for nanoparticles synthesis, or complete reduction of metal salt to nanoparticles took place at this temperature.[44,45] Temperature is a key factor on which the size of nanoparticles was dependent.[30,46]

Stability against brine solution

The stability of nanoparticles was checked against different concentrations of brine solution. Nanoparticles were found to be stable at all concentrations of brine. Absorbance intensity increases with an increase in brine concentration. Citrate synthesized Rif-Ag-NPs were negatively charged. Increasing the concentration of brine against negatively charged surface nanoparticles resulted in an increase in electrostatic interaction between Na^{+} ion and nanoparticles surface.[47] These increased electrostatic interactions then resulted in shielding of the anoparticles surface and attributing greater stability to negatively charged nanoparticles in brine solution.[48] Rifampicin conjugated silver nanoparticles were synthesized using sodium citrate, so they were negatively charged and possessed stability against all concentrations of brine, as shown in Figure 5.

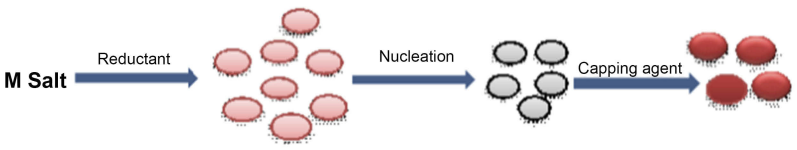

Figure 2 Capping action of rifampicin with silver nanoparticles.

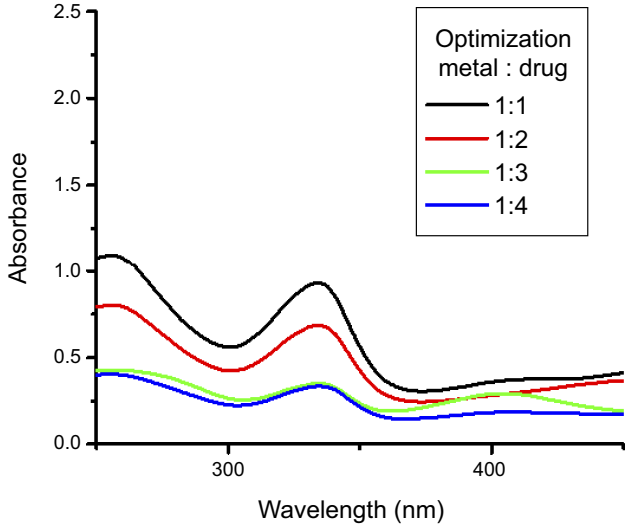

Figure 3 Reaction optimization of rifampicin conjugated silver (Rif-Ag) nanoparticles.

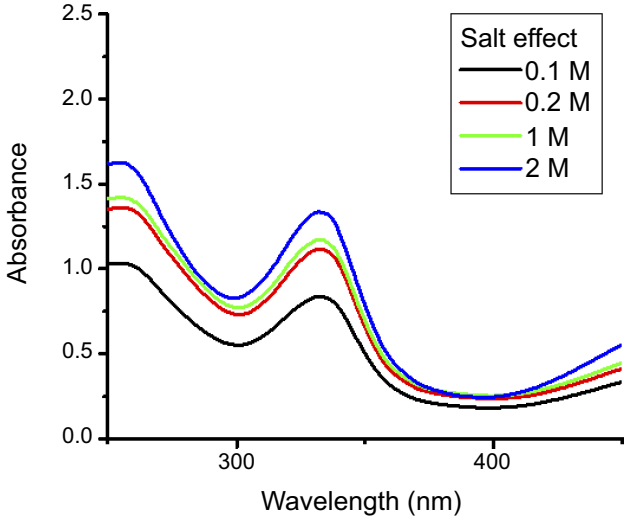

Figure 5 Stability of rifampicin conjugated silver (Rif-Ag) against brine solution.

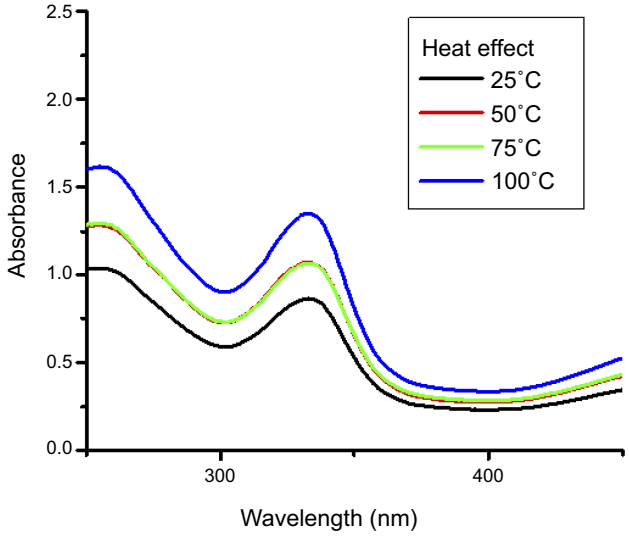

Figure 4 Heat effect on synthesis of nanoparticles.

Stability at different ranges of pH

Nanoparticles are sensitive to environmental change, and changing the pH of silver or gold nanoparticles will have a pronounced effect on particle size and surface charge.[48] Nanoparticles of various sizes and shapes can be synthesized by altering the pH of reaction medium, as the reduction activity of citrate depends upon pH of medium.[49] An increase in pH causes a corresponding increase in citrate activity.[50] The nanoparticle itself was found to be acidic in nature, having a pH of 4–5. In the case of Rif-Ag nanoparticles, an increase in absorbance intensity with an increase in pH was also noted from pH 2–7. Red shift (black) in Rif-Ag-NPs wavelength was observed due to a decrease in particles size in extremely acidic conditions,[51] as shown in Figures 6A and B. Increasing pH from acidic neutral medium will show an increase in absorption intensity with no redshift in surface plasmon resonance (SPR). As pH of Rif-Ag-NPs solution increases from 2 to 7, nanoparticles stability also increases because of a decrease in concentration of OH^- ions.[52] In the case of rifampicin conjugated silver nanoparticles, rifampicin is acidic in nature because of the presence of phenolic functionality. In an acidic environment they accept protons from the surrounding medium and interactions between ligand and silver nanoparticles surface decreases and will result in formation of aggregates. Moreover Rif-Ag-NPs were citrate synthesized, so they were unstable in extreme acidic conditions.

FTIR analysis

FTIR spectra of rifampicin were recorded before and after formation of nanoparticles, as shown in Figure 7. In the case of rifampicin, absorption bands of –NH, -OH,-C=O (Amide group), –C=O (Keto group), and C=C- stretching bands appear at 3,483, 2,972, 1,790, 1,650, and 1,556 cm^{-1}. The peak at 3,483 cm^{-1} became broadened and showed conjugation of the –NH group to the nanoparticles surface.[53] Compounds containing hydroxy and amine functional moiety in its structure were considered best for silver and gold nanoparticles synthesis.[54,55] Sodium citrate was responsible for reduction of the amide group. The FTIR spectra of rifampicin conjugated silver nanoparticles and rifampicin are given in Table 1.

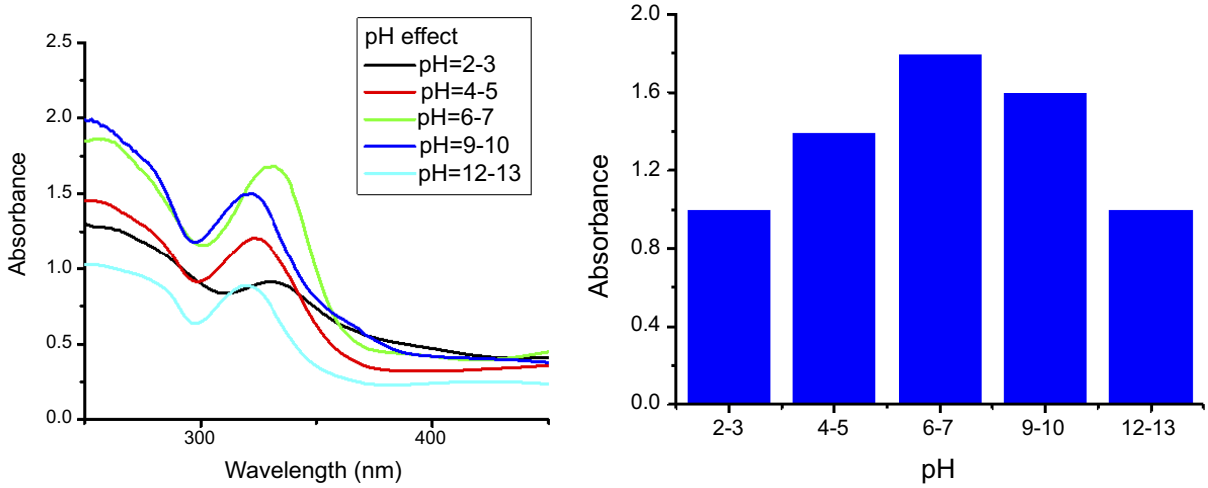

Figure 6 (**A**) pH effect on stability of rifampicin conjugated silver nanoparticles (Rif-Ag-NPs). (**B**) pH effect vs absorbance intensity.

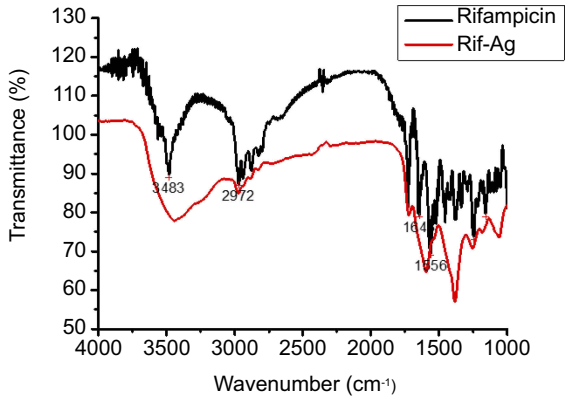

Figure 7 FTIR spectra of rifampicin and rifampicin conjugated silver (Rif-Ag) nanoparticles.

Table 1 FTIR spectra assignment of free rifampicin and Rif-Ag nanoparticles

Free Rifampicin	Rif-Ag Nanoparticles	Assignment
3,483 cm^{-1}	—	*v* (-NH)
2,972 cm^{-1}	2,972 cm^{-1}	*v* (-OH)
1,650 cm^{-1}	1,650 cm^{-1}	*v* (-C=O)
1,797 cm^{-1}	1,797 cm^{-1}	*v* (HN–C=O)
1,556 cm^{-1}	1,556 cm^{-1}	*v* (-C=C-)

Abbreviations: FTIR, Fourier transform infrared spectroscopy; Rif-Ag, rifampicin conjugated silver.

AFM analysis of rifampicin conjugated silver nanoparticles

Atomic force microscopy (AFM) was used to study surface properties of Rif-Ag nanoparticles, which showed that Rif-Ag nanoparticles are of round oval shape, having an average particle size of 15±4 nm (Figure 8). AFM data was further supported by performing TEM of Rif-Ag nanoparticles. Transmission electron microscopy also confirmed the size and shape of nanoparticles and was in strong agreement with AFM results.

TEM and SEM analysis

TEM and SEM analysis were performed to study morphological properties of Rif-Ag-NPs. From TEM images we conclude that synthesized nanoparticles were polydispersed with a round oval shape with an average particle size of 18 ±4 nm. The SEM analysis revealed that particles were nearly round spherical and clumpy shaped. The average particles size of nanoparticles was found to be 15±4 nm. Figures 9A and 10 show the morphological characteristics of Rif-Ag-NPs. As particles were not round, but were irregular, then we need to make two measurements for each particle, the "minimum diameter" and the "maximum diameter". We used the area-weighted diameter for average, standard deviation, and histogram (as shown in Figure 9B).

Antibacterial and antibiofilm activities

The antibacterial activity of the free rifampicin and its nanoparticles was similar against all the strain, except *E. aerogenes* and *S. mutans*. Free rifampicin was more active against these two strains (Table 2). Known for its penetrating power, rifampicin also showed good biofilm inhibitory and eradication activity. But the synthesized nanoparticle was found to be more potent against *K. pneumoniae, S. mutans*, and MRSA, ie, inhibits >90% biofilm at low doses as compared to rifamipicin alone. Synthesized nanoparticles significantly inhibit the biofilm formation

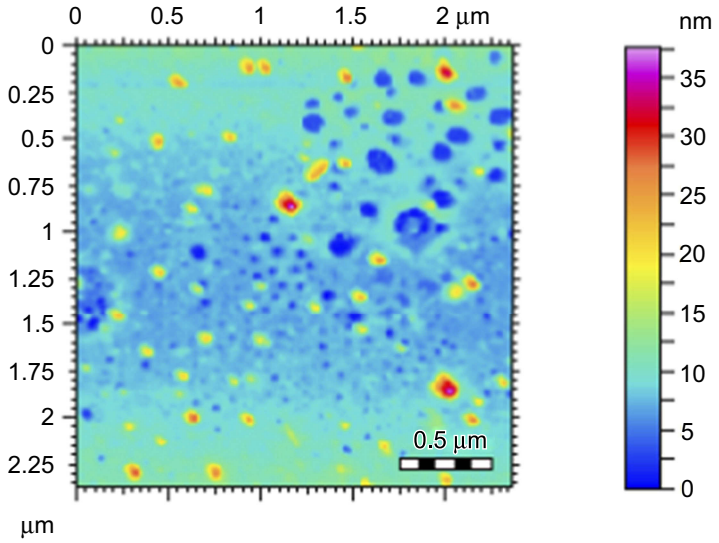

Figure 8 AFM images showing particles size distribution.

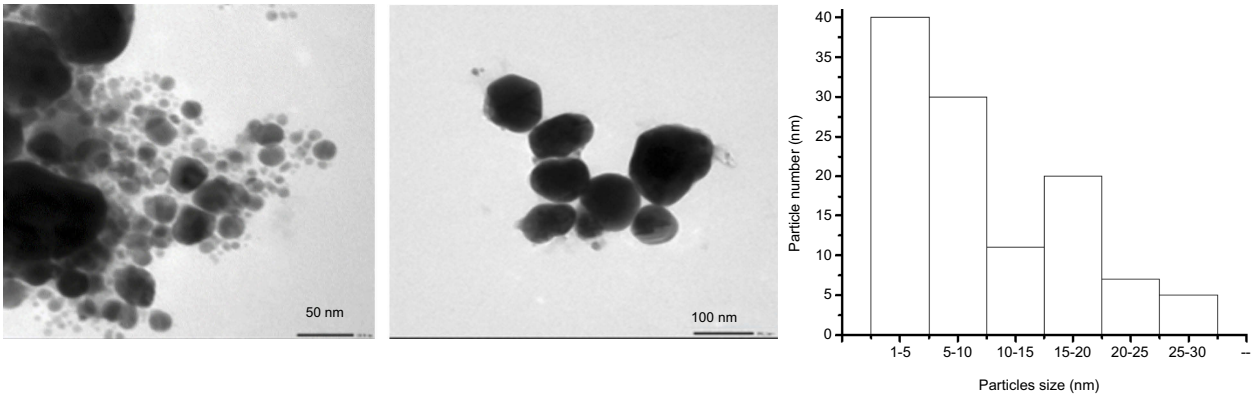

Figure 9 (**A**) TEM images of rifampicin conjugated silver (Rif-Ag) nanoparticles. (**B**) Particle size of nanoparticles distribution.

1.5-times more as compared to free rifampicin against *K. pneumoniae* and methicillin resistant *Staphylococcus aureus* (Table 2). Nanoparticles of different drugs and natural compounds have shown enhanced biofilm eradicating potential.[38] So, considering good biofilm inhibiting potential against *K. pneumoniae* and MRSA, the biofilm eradicating potential of rifampicin was also evaluated in this study against these strains and compared with rifampicin alone. Synthesized nanoparticles showed 1.5–2-times more penetrating potential as observed by biofilm eradication and percentage viability reduction as compared to rifampicin alone (Table 3; Figure 11). Our results are also in comparison to other studies which also showed the enhanced biofilm penetrating power of nanoconjugates as compared to drug alone.[56,57] So, for future studies, synthesized nanoparticles can be studied for their intracellular uptake to deal with intracellular infections and to determine the mechanism of action.

Conclusion

Rif-Ag-NPs were synthesized using a mild reducing agent such as sodium citrate using standard procedure. Other mild reducing agents such as trialkyl amine, were also used, but failed to obtain fruitful results. Spectroscopic and

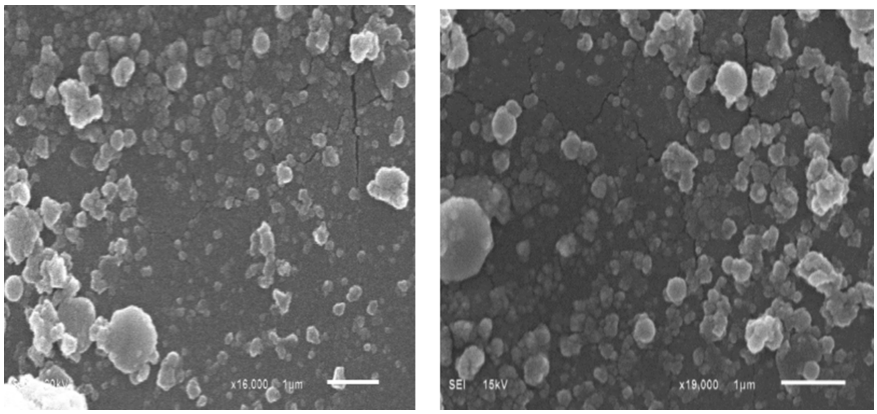

Figure 10 SEM images of rifampicin conjugated silver (Rif-Ag) nanoparticles.

Table 2 Antimicrobial and biofilm inhibition activity of raifampicin and its synthesized nanoparticle

Organisms	Rifampicin			Rifampicin nanoparticle		
	MIC (μg/mL)	MBIC (μg/mL)	Biofilm % inhibition	MIC (μg/mL)	MBIC (μg/mL)	Biofilm % inhibition
Enterobacter aerogenes	2	2	41.78±5.1	8	4	37.29±2.5
Enterococcus faecalis	8	4	46.47±2.0	8	4	31.36±1.1
Klebsiella pneumoniae	4	2	66.45±8.2	4	1	94.65±1.1***
Proteus mirabilis	4	4	44.6±3.3	4	4	28.6±2.0
Streptococcus mutans	0.05	0.1	92.46±0.8	0.2	0.1	90.6±2.1
Methicillin Resistant *Staphylococcus aureus*	0.012	0.003	64.94±2.5	0.025	0.003	93.53±0.2***

Notes: ***Statistically significant ($P<0.05$) as compared to free rifampicin.
Abbreviations: MBIC, minimum biofilm inhibitory concentration; MIC, minimum inhibitory concentration.

Table 3 Preformed biofilm eradication capability of rifampicin and its synthesized nanoparticle

Organisms	Rifampicin			Rifampicin nanoparticle		
	Biofilm eradication dose (μg/mL)	Biofilm (%) eradication	Biofilm viability (%) reduction	Biofilm eradication dose (μg/mL)	Biofilm (%) eradication	Biofilm viability (%) reduction
Klebsiella pneumoniae	10	26.3±3.8	20.37±1.2	1	40.25±0.9**	52.12±1.7***
Methicillin Resistant *Staphylococcus aureus*	1	52.69±6.2	33.62±0.5	1	69.21±1.4***	49.71±0.98**

Note: **$P<0.01$, ***$P<0.001$.

spectrometry techniques were performed for characterization of Rif-Ag nanoparticles. FTIR spectra proved conjugation of –OH and $–NH_2$ functional moiety to silver nanoparticles, while TEM and AFM images revealed that nanoparticles were round oval in shape with an average particle size of 18±4 nm. Furthermore, synthesized rifampicin capped silver nanoparticles were water-soluble and less toxic. Antibiofilm activity of Rif-Ag-NPs was checked against certain species of bacterial pathogens. A considerable increase in antibiofilm activity was observed for Rif-Ag-NPs. Microscopic images of rifampicin nanoparticle showed more inhibition at a higher dose of rifampicin. Rifampicin and its nanoparticles were most active against *Streptococcus mutans* and MRSA at lowest concentrations. Moreover, rifampicin was found to be moderately active and its nanoparticle highly active against *K. pneumoniae*.

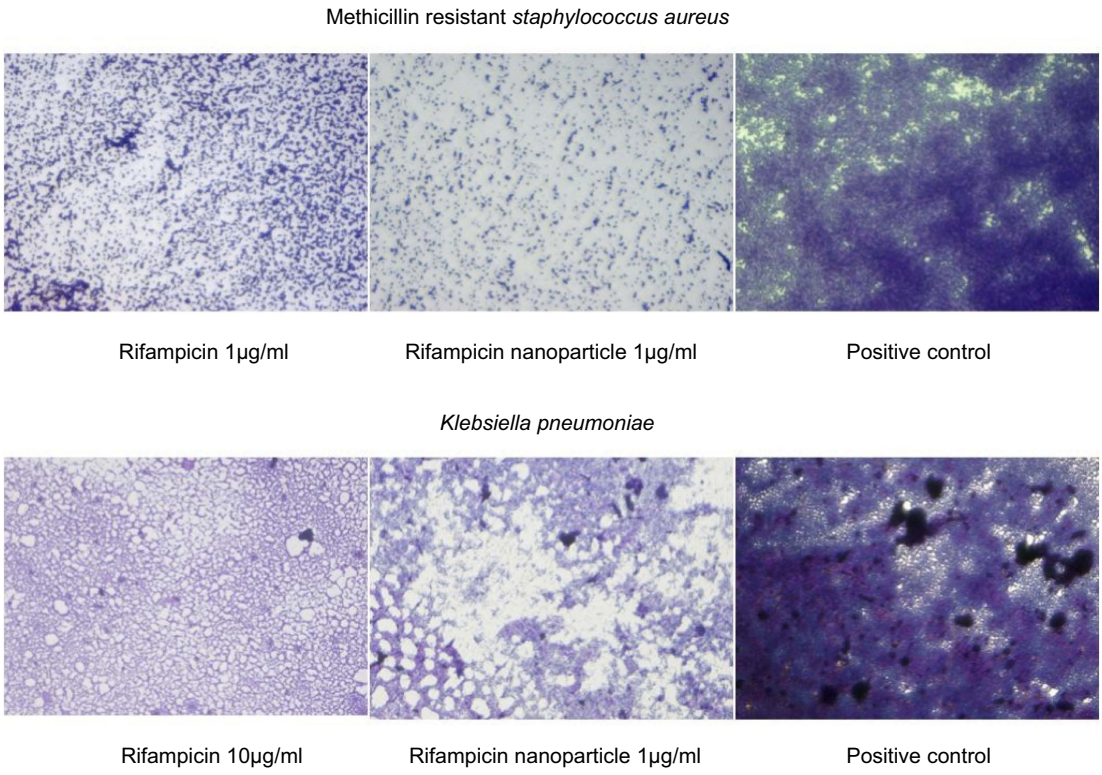

Figure 11 Biofilm eradicating potential of rifampicin and its nanoparticle.

Disclosure

The authors declare no conflicts of interest in this work.

References

1. Maekawa K, Yamasaki K, Niizeki T, et al. Drop-on-demand laser sintering with silver nanoparticles for electronics packaging. *IEEE T Comp Pack Man*. 2012;2:868–877.
2. Lorenz C, Von Goetz N, Scheringer M, Wormuth M, Hungerbühler K. Potential exposure of German consumers to engineered nanoparticles in cosmetics and personal care products. *Nanotoxicology*. 2011;5:12–29. doi:10.3109/17435390.2010.484554
3. Aricò AS, Bruce P, Scrosati B, Tarascon J-M, Van Schalkwijk W. Nanostructured materials for advanced energy conversion and storage devices. *Nat Mater*. 2005;4:366–377. doi:10.1038/nmat1368
4. Kamat PV. Meeting the clean energy demand: nanostructure architectures for solar energy conversion. *J Phys Chem C*. 2007;1:11–12.
5. Astruc D. *Nanoparticles and Catalysis*. Weinheim: John Wiley & Sons; 2008.
6. Johnson BF. Nanoparticles in catalysis. *Top Catal*. 2003;24:147–159. doi:10.1023/B:TOCA.0000003086.83434.b6
7. Sun C, Lee JS, Zhang M. Magnetic nanoparticles in MR imaging and drug delivery. *Adv Drug Deliv Rev*. 2008;60:1252–1265. doi:10.1016/j.addr.2008.03.018
8. Panyam J, Labhasetwar V. Biodegradable nanoparticles for drug and gene delivery to cells and tissue. *Adv Drug Deliv Rev*. 2003;55:329–347.
9. Corma A, Garcia H. Supported gold nanoparticles as catalysts for organic reactions. *Chem Soc Rev*. 2008;37:2096–2126. doi:10.1039/b707314n
10. Sýkora D, Kašička V, Mikšík I, et al. Application of gold nanoparticles in separation sciences. *J Sep Sci*. 2010;33:372–387. doi:10.1002/jssc.200900677
11. Zhang H, Chhowalla M, Liu Z. 2D nanomaterials: graphene and transition metal dichalcogenides. *Chem Soc Rev*. 2018;47:3015–3017. doi:10.1039/c8cs90048e
12. Nie S, Emory SR. Probing single molecules and single nanoparticles by surface-enhanced Raman scattering. *Science*. 1997;275:1102–1106.
13. Lin Q-Y, Palacios E, Zhou W, et al. DNA-mediated size-selective nanoparticle assembly for multiplexed surface encoding. *Nano Lett*. 2018;18:2645–2649. doi:10.1021/acs.nanolett.8b00509
14. Sintubin L, De Windt W, Dick J, et al. Lactic acid bacteria as reducing and capping agent for the fast and efficient production of silver nanoparticles. *Appl Microbiol Biotechnol*. 2009;84:741–749. doi:10.1007/s00253-009-2032-6
15. Gandubert VJ, Lennox RB. Assessment of 4-(dimethylamino) pyridine as a capping agent for gold nanoparticles. *Langmuir*. 2005;21:6532–6539. doi:10.1021/la050195u
16. Corbierre MK, Cameron NS, Sutton M, Laaziri K, Lennox RB. Gold nanoparticle/polymer nanocomposites: dispersion of nanoparticles as a function of capping agent molecular weight and grafting density. *Langmuir*. 2005;21:6063–6072. doi:10.1021/la047193e
17. Wang S, Chen KJ, Wu TH, et al. Photothermal effects of supramolecularly assembled gold nanoparticles for the targeted treatment of cancer cells. *Angew Chem Int Ed Engl*. 2010;49:3777–3781. doi:10.1002/anie.201000062
18. Lu L, Sun R, Chen R, et al. Silver nanoparticles inhibit hepatitis B virus replication. *Antivir Ther*. 2008;13:253.
19. Daisy P, Saipriya K. Biochemical analysis of Cassia fistula aqueous extract and phytochemically synthesized gold nanoparticles as hypoglycemic treatment for diabetes mellitus. *Int J Nanomed*. 2012;7:1189–1202. doi:10.2147/IJN.S26650
20. Alexis F, Pridgen E, Molnar LK, Farokhzad OC. Factors affecting the clearance and biodistribution of polymeric nanoparticles. *Mol Pharm*. 2008;5:505–515. doi:10.1021/mp800051m

21. Girdhar V, Patil S, Banerjee S, Singhvi G. Nanocarriers for drug delivery: mini review. *Curr Nanomed*. 2018;8:88–99. doi:10.2174/2468187308666180501092519
22. Kim SY, Lee YM. Taxol-loaded block copolymer nanospheres composed of methoxy poly (ethylene glycol) and poly (ε-caprolactone) as novel anticancer drug carriers. *Biomaterials*. 2001;22:1697–1704.
23. Mishra SS, Banode KB, Belgamwar VS. *Nanotechnology: A Tool for Targeted Drug Delivery*. Nanotechnology Applied To Pharmaceutical Technology. Alves dos Santos C, editor. Gewerbestrasse: Springer; 2017:113–137.
24. Elechiguerra JL, Burt JL, Morones JR, et al. Interaction of silver nanoparticles with HIV-1. *J Nanobiotechnol*. 2005;3:1–10. doi:10.1186/1477-3155-3-6
25. Leroux J-C, Allémann E, De Jaeghere F, Doelker E, Gurny R. Biodegradable nanoparticles—from sustained release formulations to improved site specific drug delivery. *J Control Release*. 1996;39:339–350. doi:10.1016/0168-3659(95)00164-6
26. Bobo D, Robinson KJ, Islam J, Thurecht KJ, Corrie SR. Nanoparticle-based medicines: a review of FDA-approved materials and clinical trials to date. *Pharm Res*. 2016;33:2373–2387. doi:10.1007/s11095-016-1958-5
27. Kotcherlakota R, Das S, Patra CR. *Therapeutic Applications of Green-Synthesized Silver Nanoparticles*. Green Synthesis, Characterization and Applications of Nanoparticles. Oxford: Elsevier; 2019:389–428.
28. Hayat MA. *Colloidal Gold: Principles, Methods, and Applications*. New York: Elsevier; 2012.
29. Khan JA, Kudgus RA, Szabolcs A, et al. Designing nanoconjugates to effectively target pancreatic cancer cells in vitro and in vivo. *PLoS One*. 2011;6:e20347. doi:10.1371/journal.pone.0020347
30. Pillai ZS, Kamat PV. What factors control the size and shape of silver nanoparticles in the citrate ion reduction method? *J Phys Chem B*. 2004;108:945–951. doi:10.1021/jp037018r
31. Campbell EA, Korzheva N, Mustaev A, et al. Structural mechanism for rifampicin inhibition of bacterial RNA polymerase. *Cell*. 2001;104:901–912.
32. Sensi P. History of the development of rifampin. *Rev Infect Dis*. 1983;5:S402–S406. doi:10.1093/clinids/5.Supplement_3.S402
33. Osmon DR, Berbari EF, Berendt AR, et al. Diagnosis and management of prosthetic joint infection: clinical practice guidelines by the Infectious Diseases Society of America. *Clin Infect Dis*. 2012;56:e1–e25. doi:10.1093/cid/cis803
34. Dunne W, Mason E, Kaplan SL. Diffusion of rifampin and vancomycin through a Staphylococcus epidermidis biofilm. *Antimicrob Agents Chemother*. 1993;37:2522–2526.
35. Zheng Z, Stewart PS. Penetration of rifampin through Staphylococcus epidermidis biofilms. *Antimicrob Agents Chemother*. 2002;46:900–903.
36. J-I S, Fujino T, Araake M, et al. Emergence of rifampicin resistance in methicillin-resistant Staphylococcus aureus in tuberculosis wards. *J Infect Chemother*. 2006;12:47–50. doi:10.1007/s10156-005-0417-8
37. Mu H, Guo F, Niu H, Liu Q, Wang S, Duan J. Chitosan improves anti-biofilm efficacy of gentamicin through facilitating antibiotic penetration. *Int J Mol Sci*. 2014;15:22296–22308. doi:10.3390/ijms151222296
38. Ahmed A, Khan AK, Anwar A, Ali SA, Shah MR. Biofilm inhibitory effect of chlorhexidine conjugated gold nanoparticles against Klebsiella pneumoniae. *Microb Pathog*. 2016;98:50–56. doi:10.1016/j.micpath.2016.06.016
39. Turkevich J, Stevenson PC, Hillier J. A study of the nucleation and growth processes in the synthesis of colloidal gold. *Faraday Discuss*. 1951;11:55–75. doi:10.1039/df9511100055
40. *Clinical and Laboratory Standards Institute. M27-A3: Reference Method for Broth Dilution Antifungal Susceptibility Testing of Yeasts; Approved Standard; 3rd ed*. Wayne, PA: CLSI; 2008.
41. O'Toole GA, Pratt LA, Watnick PI, Newman DK, Weaver VB, Kolter R. Genetic approaches to study of biofilms. *Methods Enzymol*. 1999;310:91–109. doi: 10.1016/S0076-6879(99)10008-9
42. Khan AK, Ahmed A, Hussain M, et al. Antibiofilm potential of 16-oxo-cleroda-3, 13 (14) E-diene-15 oic acid and its five new γ-amino γ-lactone derivatives against methicillin resistant Staphylococcus aureus and Streptococcus mutans. *Eur J Med Chem*. 2017;138:480–490. doi:10.1016/j.ejmech.2017.06.065
43. Nanda K, Maisels A, Kruis F, Fissan H, Stappert S. Higher surface energy of free nanoparticles. *Phys Rev Lett*. 2003;91:106102. doi:10.1103/PhysRevLett.91.106102
44. Qiu L, Shao Z, Yang M, et al. Study on effects of carboxymethyl cellulose lithium (CMC-Li) synthesis and electrospinning on high-rate lithium ion batteries. *Cellulose*. 2014;21:615–626. doi:10.1007/s10570-013-0108-z
45. Liu H, Zhang H, Wang J, Wei J. Effect of temperature on the size of biosynthesized silver nanoparticle: deep insight into microscopic kinetics analysis. *Arab J Chem*. Epub 2017 Sept 17.
46. Hebeish A, El-Rafie M, Abdel-Mohdy F, Abdel-Halim E, Emam HE. Carboxymethyl cellulose for green synthesis and stabilization of silver nanoparticles. *Carbohydr Polym*. 2010;82:933–941. doi:10.1016/j.carbpol.2010.06.020
47. Barton J, Pretty J. What is the best dose of nature and green exercise for improving mental health? A multi-study analysis. *Environ Sci Technol*. 2010;44:3947–3955. doi:10.1021/es903183r
48. Jiang J, Oberdörster G, Biswas P. Characterization of size, surface charge, and agglomeration state of nanoparticle dispersions for toxicological studies. *J Nanopart Res*. 2009;11:77–89. doi:10.1007/s11051-008-9446-4
49. Du X, Wang C, Chen M, Jiao Y, Wang J. Electrochemical performances of nanoparticle Fe3O4/activated carbon supercapacitor using KOH electrolyte solution. *J Phys Chem C*. 2009;113:2643–2646.
50. Ji X, Song X, Li J, Bai Y, Yang W, Peng X. Size control of gold nanocrystals in citrate reduction: the third role of citrate. *J Am Chem Soc*. 2007;129:13939–13948. doi:10.1021/ja074447k
51. Dong X, Ji X, Wu H, et al. Shape control of silver nanoparticles by stepwise citrate reduction. *J Phys Chem C*. 2009;113:6573–6576.
52. Mulvaney P, Linnert T, Henglein A. Surface chemistry of colloidal silver in aqueous solution: observations on chemisorption and reactivity. *J Phys Chem C*. 1991;95:7843–7846. doi:10.1021/j100173a053
53. Naz SS, Islam NU, Shah MR, et al. Enhanced biocidal activity of Au nanoparticles synthesized in one pot using 2, 4-dihydroxybenzene carbodithioic acid as a reducing and stabilizing agent. *J Nanobiotechnol*. 2013;11:13. doi:10.1186/1477-3155-11-13
54. Kanaras AG, Kamounah FS, Schaumburg K, Kiely CJ, Brust M. Thioalkylated tetraethylene glycol: a new ligand for water soluble monolayer protected gold clusters. *Chem Comm*. 2002;2294–2295. doi:10.1039/b207838b
55. Yang Y, Cui J, Zheng M, et al. One-step synthesis of amino-functionalized fluorescent carbon nanoparticles by hydrothermal carbonization of chitosan. *Chem Comm*. 2012;48:380–382. doi:10.1039/c1cc15678k
56. Ramos MADS, Da Silva PB, Spósito L, et al. Nanotechnology-based drug delivery systems for control of microbial biofilms: a review. *Int J Nanomed*. 2018;13:1179. doi:10.2147/IJN.S177627
57. Sabaeifard P, Abdi-Ali A, Gamazo C, Irache JM, Soudi MR. Improved effect of amikacin-loaded poly (D, L-lactide-co-glycolide) nanoparticles against planktonic and biofilm cells of Pseudomonas aeruginosa. *J Med Microbiol*. 2017;66:137–148. doi:10.1099/jmm.0.000430